

Dirac eigenvalues and eigenvectors at finite temperature*

M. Göckeler^a, H. Hehl^a, P.E.L. Rakow^a, A. Schäfer^a, W. Söldner^a, and T. Wettig^b

^aInstitut für Theoretische Physik, Universität Regensburg, D-93040 Regensburg, Germany

^bCenter for Theoretical Physics, Yale University, New Haven, CT 06520-8120, USA and
RIKEN BNL Research Center, Brookhaven National Laboratory, Upton, NY 11973-5000, USA

We investigate the eigenvalues and eigenvectors of the staggered Dirac operator in the vicinity of the chiral phase transition of quenched SU(3) lattice gauge theory. We consider both the global features of the spectrum and the local correlations. In the chirally symmetric phase, the local correlations in the bulk of the spectrum are still described by random matrix theory, and we investigate the dependence of the bulk Thouless energy on the simulation parameters. At and above the critical point, the properties of the low-lying Dirac eigenvalues depend on the Z_3 -phase of the Polyakov loop. In the real phase, they are no longer described by chiral random matrix theory. We also investigate the localization properties of the Dirac eigenvectors in the different Z_3 -phases.

1. INTRODUCTION

The theoretical understanding of the Dirac spectrum has improved considerably in the past few years. Using a variety of methods such as finite volume partition functions [1], partially quenched chiral perturbation theory [2], and chiral random matrix theory (RMT) [3], it has been shown that in the phase in which chiral symmetry is spontaneously broken, the distribution and the correlations of the low-lying Dirac eigenvalues are described by relatively simple universal functions. This description is valid in a regime in which the zero-momentum modes dominate the effective Lagrangian. The energy scale which limits this regime is known as the Thouless energy. For a review, we refer to Ref. [4].

Recently, two studies [5,6] have appeared in which the Dirac spectrum was investigated in this context for temperatures T close to the critical temperature T_c of the chiral phase transition. This is an interesting problem, since the above-mentioned approach only works in the broken phase, and one would like to find out what happens to the universal features as one crosses T_c . The present study addresses these and related questions. In addition, we also investigate the properties of the Dirac eigenvectors.

2. Z_3 ENSEMBLES

We are working in the quenched approximation using the staggered discretization of the Dirac operator. In a study of chiral symmetry restoration in the quenched approximation, an interesting observation was made in Ref. [7]. The gauge action has a Z_3 symmetry (for $N_c = 3$ colors) which is broken in the deconfinement phase. As a result, the phases of the Polyakov loop P cluster around the elements of Z_3 in the complex plane, and one can divide the total ensemble of gauge field configurations into three classes with $\arg(P) = 0, \pm 2\pi/3$. An example is shown in Fig. 1. It was found [7] that the chiral condensate computed from the class of configurations with $\arg(P) = 0$ vanishes above T_c as expected. However, for $\arg(P) = \pm 2\pi/3$ it remains nonzero in a certain range of T above T_c . This behavior can be understood qualitatively in NJL-type models [8,9] and in RMT [10]. The point is that the boundary conditions of the Dirac operator are not invariant under Z_3 transformations, and for $\arg(P) = \pm 2\pi/3$, the new boundary conditions lead to a shift of the Dirac eigenvalues to lower values [10]. Using the Banks-Casher relation [11], this implies a nonzero chiral condensate.

In the following analysis, we therefore separate our configurations into two ensembles, those with $\arg(P) = 0$ (ensemble E1) and those with

*Presented by TW at Lattice 2000, Bangalore, India.

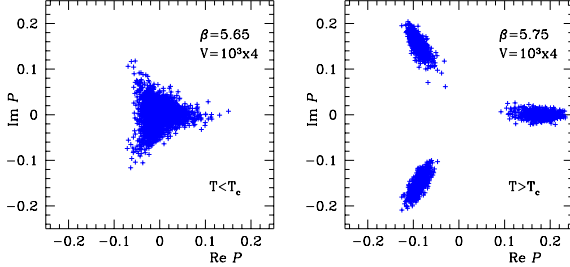


Figure 1. Scatter plot of the Polyakov loop in the complex plane in the confinement (left) and deconfinement (right) phase.

$\arg(P) = \pm 2\pi/3$ (ensemble E2), respectively. This separation can be done unambiguously. For the purpose of the present analysis, the two classes $\arg(P) = \pm 2\pi/3$ are equivalent and can be combined in E2. In full QCD, the fermion determinant suppresses the E2 configurations. (In Ref. [6], the E2-configurations were Z_3 -rotated before the Dirac operator was diagonalized so that $\arg(P) = 0$ in their analysis [12].)

Strictly speaking, we should distinguish three critical temperatures, T_d for the deconfinement phase transition, and T_{c1} and T_{c2} for the chiral phase transitions of E1 and E2, respectively. Here, we assume that $T_d \approx T_{c1}$. Since we are mainly interested in the region $T \approx T_{c1}$, we write T_c instead of T_{c1} in the following.

3. DIRAC SPECTRUM

We have worked on $N_s^3 \times N_t$ lattices with $N_t=4$ and 6 for which $\beta_c(N_s \rightarrow \infty)=5.6925$ and 5.8941, respectively [13]. An example for the global spectral density of the Dirac operator near zero for $T \gtrsim T_c$ is shown in Fig. 2. For the E1-ensemble,

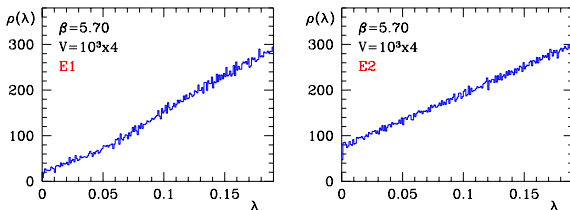


Figure 2. Global spectral density of the Dirac operator at $T \gtrsim T_c$ for the two different ensembles.

we find $\rho(0) \approx 0$ which, according to the Banks-Casher relation, implies that chiral symmetry is restored. On the other hand, for E2 we observe that $\rho(0) \neq 0$ which implies a nonzero chiral condensate, in agreement with [7].

We therefore expect the distribution of the low-lying Dirac eigenvalues to be different in the two ensembles. Here, we concentrate on the smallest positive eigenvalue, λ_{\min} . Depending on whether or not $\langle \bar{\psi}\psi \rangle \neq 0$, the expectation value $\langle \lambda_{\min} \rangle$ scales as follows:

$$\begin{aligned} T < T_c : \quad \lambda_{\min} &\sim V^{-1}, \\ T > T_c : \quad \lambda_{\min} &\sim V^0, \\ T = T_c : \quad \lambda_{\min} &\sim V^{-\delta/(\delta+1)}, \end{aligned} \quad (1)$$

where δ is one of the universal critical exponents of a second order phase transition. For $T < T_c$, the distribution of λ_{\min} is described by the RMT result, $P(\lambda_{\min}) = (c^2 \lambda_{\min}/2) \exp(-c \lambda_{\min}^2/4)$ with $c = V |\langle \bar{\psi}\psi \rangle|$. At $T = T_c$, RMT predictions for $P(\lambda_{\min})$ [14] are model dependent.

Our results for $P(\lambda_{\min})$, along with fits to the RMT prediction in the broken phase, are shown in Fig. 3. As expected, the results for the two ensembles E1 and E2 are very different. The top figure corresponds to $T \approx T_c$, and the bottom figure to T slightly above T_c . In both figures, $\langle \lambda_{\min} \rangle$ is much larger in E1 than in E2. This reflects the fact that in the symmetric phase, small eigenvalues are suppressed. Also, $P(\lambda_{\min})$ in E1 is clearly not described by the RMT prediction (which is valid for $T < T_c$). For E2 at $T \approx T_c$, however, $P(\lambda_{\min})$ is still very well described by RMT, consistent with the fact that chiral symmetry is still broken for this ensemble. For $T > T_c$ the agreement becomes worse.

Other quantities such as the microscopic density could be analyzed in exactly the same way, and the results and conclusions will be similar.

4. THOULESS ENERGY FOR $T > T_c$

The Thouless energy [15] is the limiting energy above which the universal description of the Dirac spectrum in terms of RMT is no longer valid. One has to distinguish between the Thouless energy at the hard edge and in the bulk of the spec-

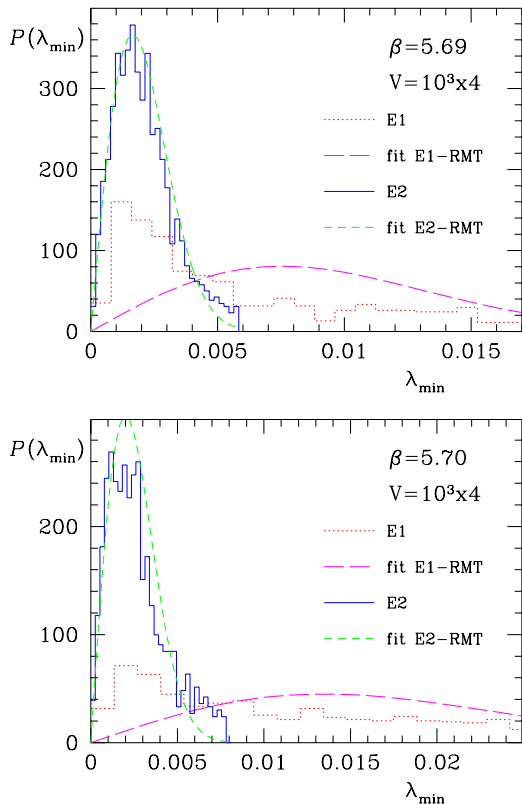


Figure 3. Distribution of the smallest Dirac eigenvalue (from 2000 configurations) in the two ensembles for $T \approx T_c$ (top) and $T \gtrsim T_c$ (bottom).

trum. The Thouless energy at the hard edge is very well understood, both theoretically [16] and on the lattice [17]. For $T > T_c$ the hard edge is no longer described by RMT so that the concept of a Thouless energy no longer exists. However, in the bulk the local spectral correlations are still given by RMT, and it is interesting to study the bulk Thouless energy above T_c . A convenient measure of the bulk spectral correlations is the number variance defined by

$$\Sigma^2(L) = \langle (n(L) - \langle n(L) \rangle)^2 \rangle, \quad (2)$$

where $n(L)$ is the number of levels in an interval of length L after the spectrum has been unfolded. There are several questions related to how the spectrum should be unfolded, see Ref. [18] for a comprehensive discussion. We have used ensemble averaging to construct the average spec-

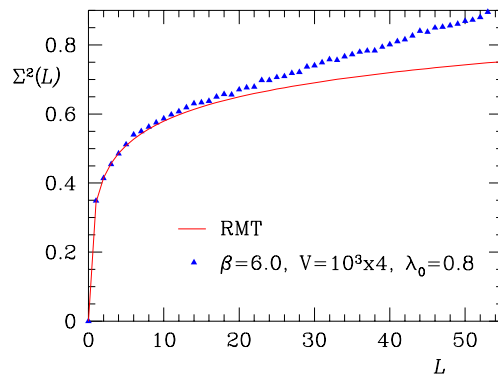


Figure 4. Number variance of the Dirac eigenvalues in the bulk of the spectrum. λ_0 is the starting point of the interval of length L .

tral density used in the unfolding procedure. The number variance was also computed by ensemble averaging. A typical example for $\Sigma^2(L)$, averaged over 600 independent configurations, is shown in Fig. 4, along with the parameter-free prediction of RMT. We observe that for small values of L , the lattice data are nicely described by RMT. We also see that there is a critical scale L_c , the Thouless scale, above which nonuniversal behavior sets in. In order to extract this scale from the data, we construct the ratio

$$\text{ratio}(L) = \frac{\Sigma_{\text{latt}}^2(L) - \Sigma_{\text{RMT}}^2(L)}{\Sigma_{\text{RMT}}^2(L)} \quad (3)$$

which should start to deviate strongly from 0 above L_c . We find that the numerical value of the Thouless scale depends on where we are in the spectrum, i.e., on the starting point of the interval of length L . This means that spectral averaging must not be used to construct $\Sigma^2(L)$ for the purpose of extracting the Thouless energy.

In Fig. 5, we show the ratio of Eq. (3) for two different starting points, $\lambda_0 = 0.5$ and $\lambda_0 = 0.8$, and for various lattice sizes at $\beta = 6.0$, which is above β_c for both values of N_t . Again, we used 600 independent configurations per parameter set. We observe that the Thouless scale seems to be independent of N_s , but depends on N_t . We are currently investigating the form of this N_t dependence.

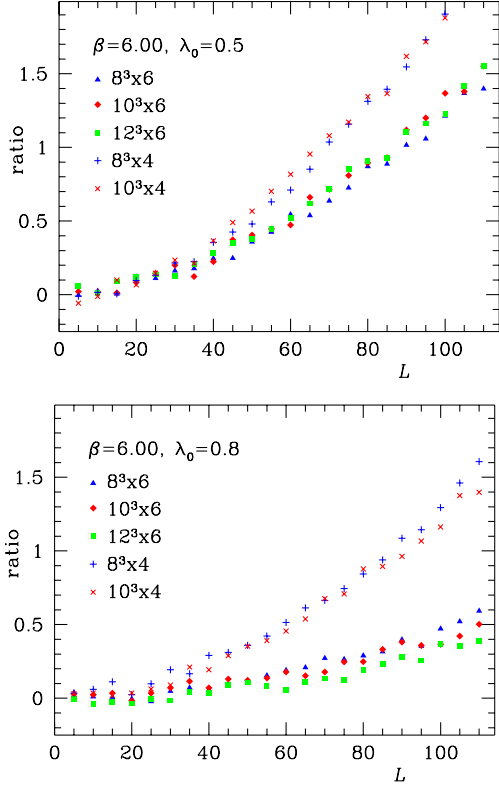


Figure 5. The ratio defined in Eq. (3) for two different values of λ_0 and various lattice sizes.

5. LOCALIZATION PROPERTIES OF DIRAC EIGENVECTORS

In condensed matter physics, the question of whether or not a disordered mesoscopic sample is a metal or an insulator can be answered by constructing the so-called inverse participation ratio I_2 , which is a measure of how many sites contribute significantly to the wave function. For the case of QCD, we introduce the gauge-invariant definition

$$I_2(\lambda) \equiv V \frac{\sum_x p_\lambda(x)^2}{[\sum_x p_\lambda(x)]^2}, \quad (4)$$

where V is the lattice volume and $p_\lambda(x)$ is the gauge-invariant probability density

$$p_\lambda(x) = \sum_{\alpha=1}^{N_c} |\psi_\lambda^\alpha(x)|^2. \quad (5)$$

Here, x denotes a lattice site, α is a color index, and $\psi_\lambda^\alpha(x)$ is a component of the eigenvector corresponding to eigenvalue λ . Because of chiral symmetry we have $\sum_{x \text{ even}} p_\lambda(x) = \sum_{x \text{ odd}} p_\lambda(x)$. A completely localized state therefore has $I_2 = V/2$. This case corresponds to uncorrelated eigenvalues and is described by the Poisson ensemble. (The corresponding mesoscopic sample would be an insulator.) For a completely delocalized state, $p_\lambda(x)$ is the same for all x , and $I_2 = 1$. In RMT, we find

$$\langle I_2 \rangle = \left(1 + \frac{1}{N_c}\right) \frac{N_c V}{N_c V + 2} \xrightarrow{V \rightarrow \infty} 1 + \frac{1}{N_c}. \quad (6)$$

This case corresponds to extended wave functions with many significant components and strongly correlated eigenvalues. (The corresponding mesoscopic sample would be a metal.) In QCD, a simple argument (see [4]) shows that if chiral symmetry is broken, the Dirac wave functions must be extended.

Our results for the inverse participation ratio of the low-lying Dirac eigenvectors are shown in Fig. 6. Several features are worth noting:

1. Below T_c all eigenvectors are extended, which is consistent with the fact that the eigenvalues are described by RMT both at the hard edge and in the bulk of the spectrum. The eigenvectors corresponding to smaller eigenvalues are slightly more “localized” than those corresponding to larger eigenvalues. The data agree well with the RMT prediction, $\langle I_2 \rangle = 4/3$, for large $\langle \lambda \rangle$. In contrast to the observation of Ref. [19] for Wilson fermions, we did not find signs of strong localization.
2. The eigenvectors corresponding to eigenvalues in the bulk of the spectrum remain extended for E1 and E2 at all temperatures considered, consistent with the fact that the eigenvalues in the bulk continue to be described by RMT above T_c .
3. Most interestingly, the eigenvectors of the E1 ensemble corresponding to the lowest eigenvalues become more localized at and above T_c , while in the E2 sector the lowest eigenmodes remain extended.

We are currently studying the topological properties of the low-lying eigenvectors and will present our results in the near future.

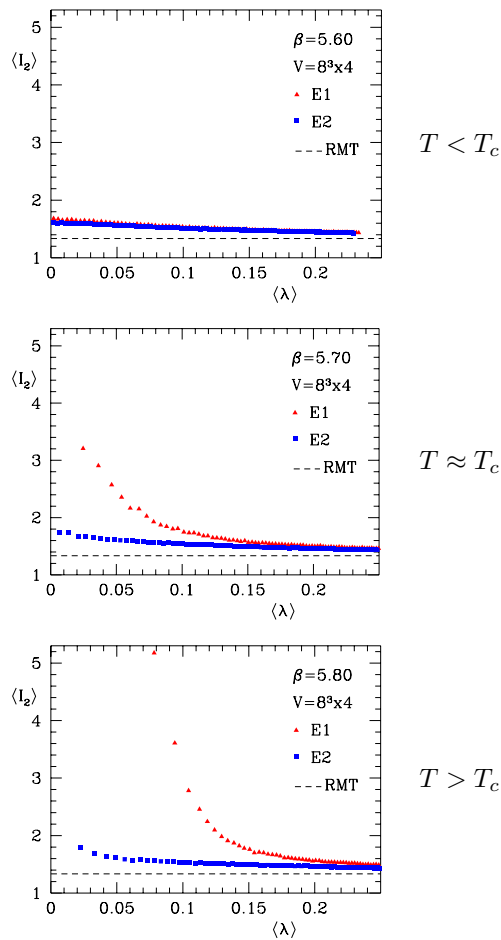


Figure 6. Average inverse participation ratio $\langle I_2 \rangle$ of the low-lying Dirac eigenvectors vs average eigenvalue in the different Z_3 -phases for temperatures below, at, and above T_c .

6. CONCLUSIONS

The behavior of the Dirac spectrum at and above the critical temperature can help to improve our understanding of the chiral phase transition. In particular, the properties of the Dirac eigenvectors deserve further study. Of course, the quenched approximation and the use of staggered fermions make it difficult to establish contact with continuum QCD. These systematic problems can be circumvented by using dynamical Ginsparg-Wilson fermions which, however, require large computational resources. For the mo-

ment, we are restricted to exploratory studies such as the present one.

Acknowledgments. This work was supported by DFG project Scha 458/5-3 and by DOE grants DE-FG02-91ER40608 and DE-AC02-98CH10886.

REFERENCES

1. H. Leutwyler and A.V. Smilga, Phys. Rev. D 46 (1992) 5607.
2. C.W. Bernard and M.F.L. Golterman, Phys. Rev. D 46 (1992) 853; J.C. Osborn, D. Toublan, and J.J.M. Verbaarschot, Nucl. Phys. B 540 (1999) 317.
3. E.V. Shuryak and J.J.M. Verbaarschot, Nucl. Phys. A 560 (1993) 306.
4. J.J.M. Verbaarschot and T. Wettig, Annu. Rev. Nucl. Part. Sci. 50 (2000) 343.
5. F. Farchioni et al., Phys. Rev. D 62 (2000) 014503.
6. P.H. Damgaard et al., Nucl. Phys. B 583 (2000) 347.
7. S. Chandrasekharan and N.H. Christ, Nucl. Phys. B (Proc. Suppl.) 47 (1996) 527.
8. P.N. Meisinger and M.C. Ogilvie, Phys. Lett. B 379 (1996) 163.
9. S. Chandrasekharan and S. Huang, Phys. Rev. D 53 (1996) 5100.
10. M.A. Stephanov, Phys.Lett. B375 (1996) 249.
11. T. Banks and A. Casher, Nucl. Phys. B 169 (1980) 103.
12. U. Heller, private communication.
13. G. Boyd et al., Nucl. Phys. B 469 (1996) 419.
14. G. Akemann et al., Nucl. Phys. B 519 (1998) 682; E. Brézin and S. Hikami, Phys. Rev. E 57 (1998) 4140; R.A. Janik et al., Phys. Lett. B 446 (1999) 9.
15. D.J. Thouless, Phys. Rep. 13 (1974) 93.
16. J.C. Osborn and J.J.M. Verbaarschot, Nucl. Phys. B 525 (1998) 738, Phys. Rev. Lett 81 (1998) 268; R.A. Janik et al., Phys. Rev. Lett. 81 (1998) 264.
17. M.E. Berbenni-Bitsch et al., Phys. Lett. B 438 (1998) 14.
18. T. Guhr et al., Phys. Rev. D 59 (1999) 054501.
19. K. Jansen and C. Liu, Nucl. Phys. B (Proc. Suppl.) 53 (1997) 974.